J Mater Sci (2017) 52:12067–12078

Biomaterials

Preparation and characterization of poly(ε-caprolactone)/ZnO foams for tissue engineering applications

Aleksandra Bužarovska[1,*]

[1] *Faculty of Technology and Metallurgy, Sts Cyril and Methodius University, Rudjer Boskovic 16, 1000 Skopje, Republic of Macedonia*

Received: 25 March 2017
Accepted: 29 June 2017
Published online: 10 July 2017

ABSTRACT

Fabrication of polymer scaffolds via various preparation procedures generally leads to creation of different morphologies, microstructure and properties. In this work, porous nanocomposite scaffolds of poly(ε-caprolactone) filled with different quantities of ZnO nanoparticles (0.5–5 wt%) were prepared by thermally induced phase separation (TIPS), using freeze-extraction method for solvent removal. The aim of this research was to investigate the influence of the fabrication procedure and the ZnO loadings on the PCL thermal, morphological and bioactivity properties. The TIPS procedure was confirmed to induce significantly high degree of crystallinity (up to 81%) in all investigated scaffolds, besides the nucleation capacity of the nanofiller. The in vitro bioactivity and biodegradability were tested by immersing produced scaffolds in standard simulated body fluid (SBF) for different periods of time (15 and 30 days). Scanning electron microscopy, Fourier transform infrared spectroscopy and X-ray diffraction were used to assess the variations in scaffolds after their incubation in SBF. No bioactivity was identified for 15 days of immersion, while the mineralization process was confirmed in all investigated scaffolds for the incubated period of 30 days. Thermogravimetric analysis was used to quantify the mineralization properties, confirming best mineralization properties in scaffolds containing lower contents of ZnO nanofiller (0.5 and 1 wt%).

Introduction

Biodegradable polymers (BP) from natural and synthetic origin have significant role in the development of new materials used for tissue engineering applications [1, 2]. In the last 20 years, they are subject of intensive research by many groups, aiming to develop polymer scaffolds with defined porosity, pore interconnectivity and adequate mechanical stability. The most important characteristic that makes these polymers attractive for tissue engineering application is their biodegradability, a process that could be time-controlled and long enough to enable

Address correspondence to E-mail: abuzar@tmf.ukim.edu.mk

DOI 10.1007/s10853-017-1342-9

generation of new tissue as a replacement for degraded scaffold [3]. The controllable biodegradability and biocompatibility of these polymers are still an imperative in the related scientific community.

Poly(ε-caprolactone) as a biodegradable polymer has received considerable scientific attention in this field, not only due to its relatively good mechanical properties, but also because of its biodegradability into non-toxic natural metabolites [4]. On the other hand, this polymer degrades significantly slow, making it less attractive for biomedical application, but more interesting as a material for long-term implant application. Otherwise, PCL has been proved as a polymer matrix with excellent potential for bone and cartilage repair, and it was successfully used as a scaffold material in various forms [5, 6].

Besides the additional positive characteristics, for example low cost and easy processability (due to its low melting temperature of around 60 °C), PCL has some disadvantages such as hydrophobicity, insufficient biocompatibility (for some tissue engineering applications), lack of functional groups necessary for cell adhesion, slow rate of degradation and insufficient mechanical strength when used as scaffold for bone tissue engineering applications [7, 8].

In order to overcome these disadvantages, PCL composites were developed comprising different kinds of ceramic particles (with micro- and nanodimensions) [9–11], metal nanoparticles [12] as well as CNTs [13]. The incorporation of micro-fillers might improve the mechanical stability of the scaffolds, but in some cases, due to the lack of bonding between the polymer and microparticles, they do act as a source of defects. More effective fillers into the biodegradable polymer matrices were identified using different nanoparticles. Based on their higher surface area, nanoparticles have significant influence on composite reinforcement (even at lower nanofiller content), topography changes and improved reception and attachment of cells, their growth and proliferation [14].

ZnO as nanofiller in PCL scaffolds has received limited attention when compared to PCL scaffolds filled with different micro- and nano-sized fillers. This nanofiller was identified as an effective biological material due to the presence of surface OH groups that could act as active sites for different cells adhesion and growth [15]. The presence of surface hydroxyl groups in many ceramic particles was proved to induce the creation of hydroxyapatite, as an important material for bioactivity evaluation [16].

According to the recent knowledge, several reports on PCL/ZnO nanocomposite membranes as biomaterials (produced by electro-spinning method) have been reported [17–19]. It was demonstrated that ZnO nanofiller induced significant metabolic activity of cells [17] and capacity to generate reactive oxygen species responsible for inducing angiogenesis [18]. Furthermore, these materials exhibited good biocompatibility in vitro. [17]. Similarly, produced PCL/ZnO electrospun membrane composites were proved to increase the biocompatibility of magnesium alloys when used as composite coatings [20].

Different methodologies for scaffolds fabrication, such as electro-spinning, gas foaming, particulate leaching and phase separation could lead to different BP morphologies, porosity, pore size and shape as well as interconnectivity [21, 22]. In thermally induced phase-separation process, the removal of frozen solvent with non-solvent extraction (usually using ethanol) besides its disinfection effect could additionally influence the morphology of the produced scaffolds [23, 24].

The aim of this paper was to produce biodegradable PCL/ZnO scaffolds using thermally induced phase-separation and freeze-extraction methods and to perform careful investigation of the thermal, morphological and bioactivity properties of PCL scaffolds from a material point of view. At the same time, a correlation between ZnO nanofiller content and above mentioned properties was determined through this research. Additionally, an attempt was made to quantify the mineralization process of PCL scaffolds in simulated body fluid (SBF) and to evaluate their degradability using Fourier transform infrared (FTIR) spectroscopy through crystallinity and carbonyl indices changes.

Experimental part

Materials and methods

PCL (Capa 6506) with molecular weight of $M_w = 50000$ g mol^{-1} was a product of Solvay, while ZnO nanoparticles (NM-110) were kindly supplied by the European Commission (JRC). Dioxane (Merck product) was used as a solvent for scaffolds preparation, and ethanol (99.5%, product of Alkaloid) was

used as medium for solvent extraction. The solvents were used without further purification.

Preparation of PCL/ZnO scaffolds

The PCL/ZnO nanocomposite scaffolds were prepared by thermally induced phase-separation method (TIPS) using freeze extraction method for solvent removal. PCL solution in dioxane at 50 °C was prepared by mechanical stirring. Appropriate content of ZnO nanofiller was previously dispersed in dioxane and ultrasonically treated for 30 min. The polymer solution was mixed together with the prepared ZnO dispersion in dioxane to obtain 5 wt% solutions with different contents of nanofiller (0.5, 1, 2 and 5 wt% related to the polymer). The resulting mixtures were additionally ultrasonically treated for additional 30 min and finally frozen at −30 °C in deep freezer. The frozen mixtures were left in the freezer for 24 h. The solvent was removed via freeze-extraction procedure with ethanol, changing the extraction solvent every 24 h subsequently during the next 3 days. The produced scaffolds were vacuum-dried at room temperature. The composition and designation of the PCL/ZnO scaffolds are summarized in Table 1.

Bioactivity and degradation in simulated body fluid

Bioactivity of the produced scaffolds was tested by immersion of the scaffolds in simulated body fluid (SBF, pH 7.25), prepared according to Kokubo [25]. The scaffolds were soaked in the prepared SBF solutions at 37 °C and were kept for 15 and 30 days. Fresh SBF solution was changed every 48 h. After completing the treatment, the scaffolds were gently washed with distilled water several times and properly vacuum-dried overnight. The samples incubated for 15 days are designated as series (I), while scaffolds soaked for 30 days are denoted as series (II).

Table 1 PCL and PCL/ZnO nanocomposite scaffolds prepared by TIPS

Sample	PCL/ZnO w/w (%)
PCL	100/0
PCL-0.5	99.5/0.5
PCL-1	99/1
PCL-2	98/2
PCL-5	95/5

Characterization of PCL/ZnO scaffolds

The porosity measurements of the produced scaffolds were taken by liquid displacement method according to Ref. [26].

Vega 3 LMV (Tescan) scanning electron microscopy (SEM) instrument was used to characterize the morphology, pores structure and pore size of the prepared nanocomposite scaffolds. The specimens for SEM observation were cut using sharp razor blade and properly coated using Q150R gold sputter coater (Quorum Technology) prior to the measurements.

Thermogravimetric analyzer (PerkinElmer, Pyris Diamond System) was used to determine the actual content of nanofiller in the corresponding PCL matrix and its thermal stability. The samples of around 10 mg were heated from 30 to 700 °C, with a heating rate of 10° min^{-1}, under constant nitrogen flow (50 cm^3 min^{-1}). Thermogravimetric analysis (TGA) measurements of treated scaffolds in SBF were taken in triple (under the same experimental conditions, explained above), and the mass residue was determined at 600 °C, as an average value of the three measurements.

DSC measurements were taken using differential scanning calorimeter (DSC Q200, TA Instruments). The PCL composites sealed in aluminum pans with weight of around 5 mg were heated from −80 to 100 °C with a heating rate of 10° min^{-1} (I run) and kept at the end temperature for 5 min. The samples were cooled to −30 °C, with a cooling rate of 10° min^{-1} (II run) and reheated up to 100 °C with a heating rate of 10° min^{-1} (III run). The crystallinity of the produced scaffolds was determined using the following equation:

$$X_c = \frac{\Delta H_m}{\Delta H_m^0 \times w_{PCL}} \times 100 \quad (1)$$

where ΔH_m is the experimental melting enthalpy, ΔH_m^0 is the melting enthalpy of 100% crystalline PCL taken as 139.5 kJ g^{-1} [27], and w_{PCL} is the PCL weight fraction in the corresponding scaffold.

An FTIR spectroscopic analysis of the prepared scaffolds was made using PerkinElmer, Spectrum 100 FTIR spectrometer (USA). FTIR–ATR spectra were recorded by accumulating 32 scans in the range of 4000–600 cm^{-1}, with resolution of 4 cm^{-1}.

X-ray analysis (XRD) was performed on a Rigaku Ultima, powder X-ray Diffractometer, with CuKα

radiation ($\lambda = 0.154$ nm). The measurements were taken in 2θ range between 5° and 60°, with scan rate of 2° min^{-1}.

Results and discussion

Thermal and structural characterization of prepared scaffolds

TGA curves of all investigated scaffolds are presented in Fig. 1. It could be noted that the degradation temperatures of the PCL composite scaffolds are shifted to lower values; 372, 366, 358 and 294 °C for the PCL-0.5, PCL-1, PCL-2 and PCL-5, respectively, when compared to degradation temperature of 383 °C for unloaded PCL scaffold. The increased content of ZnO nanofiller promotes the degradation process in the PCL foams, thus decreasing the thermal stability of the polymer matrix. The decrease in the degradation temperature observed for the loaded polymer scaffolds could be mainly due to the negative catalytic effect of the nanofiller, where surface hydroxyl groups of ZnO catalytically hydrolyze the ester groups of the PCL matrix. Similar behavior in polymer composites loaded with different nanofillers has been identified in the literature [28, 29]. The residual weights (determined at temperature of 600 °C) confirmed the nominal content of added nanofiller in each polymer scaffold (Table 2).

In order to quantify the evolved crystallinity in the polymer matrix during the scaffolds fabrication process, the DSC first melting runs were analyzed.

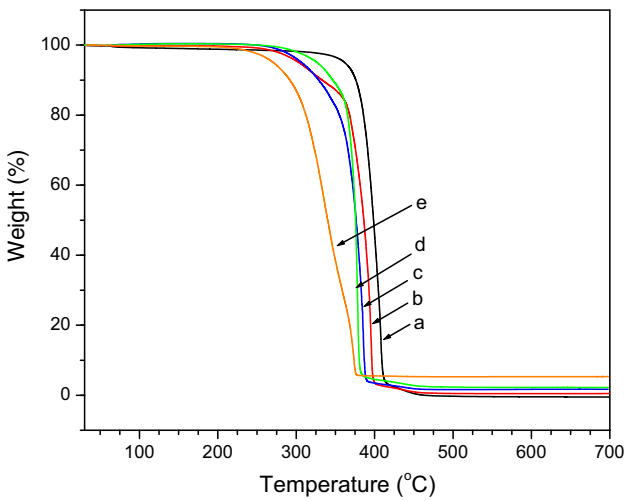

Figure 1 TGA curves of PCL (*a*), PCL-0.5 (*b*), PCL-1 (*c*), PCL-2 (*d*) and PCL-5 (*e*) scaffolds.

Table 2 Thermal properties of PCL/ZnO scaffolds, determined by thermogravimetry

Sample	T_{onset} (°C)	Residue (%)[a]	Residue (%)[b]
PCL	383	0.08	0.8 ± 0.1
PCL-0.5	372	0.49	1.92 ± 0.04
PCL-1	366	1.1	1.7 ± 0.11
PCL-2	358	1.9	1.4 ± 0.14
PCL-5	294	5.3	1.1 ± 0.09

[a] At 600 °C, for prepared scaffolds

[b] At 600 °C, for scaffolds soaked in SBF for 30 days

The DSC curves showed single melting endotherm (Fig. 2), with melting temperatures around 61 ± 1 °C, almost independent of the ZnO content, while the degree of crystallinity X_c is significantly influenced by the nanofiller loadings (Table 3). From the collected data, it could be seen that all composite scaffolds exhibit significantly higher degrees of crystallinity when compared to the X_c of pure PCL scaffold. The thermally induced phase-separation process usually leads to higher polymer crystallinity, but in this case it seems that the presence of nanofiller additionally supports the crystallization process of PCL matrix. The glass transition temperatures of all microporous PCL/ZnO scaffolds are close to the T_g value quoted for pure PCL matrix, i.e., −61 °C. This constancy in the T_g's could support the hypothesis that the no specific interactions between the nanofiller and the polymer matrix occurred [30].

The crystallization behavior from the polymer melt might give an additional view on the crystallization process of PCL matrix. From the cooling runs (Fig. 3), it could be seen that the crystallization temperatures T_c are slightly shifted to higher values with the increase in ZnO content. Additionally, the estimated degrees of crystallinity ranged between 44 and 47% for the filled scaffolds when compared to the $X_c = 38\%$ characteristic for the pure PCL scaffold (Table 3). The undercooling determined as $\Delta T = T_m - T_c$ can be used furthermore to characterize the crystallization rate of the polymer matrix. It could be underlined that the undercooling decreased with the increasing content of ZnO nanoparticles. In summary, the tendency of slight increase in crystallization temperatures and degrees of crystallinity of all filled scaffolds as well as lower values for the supercoolings support the nucleation ability of the used nanofiller [31].

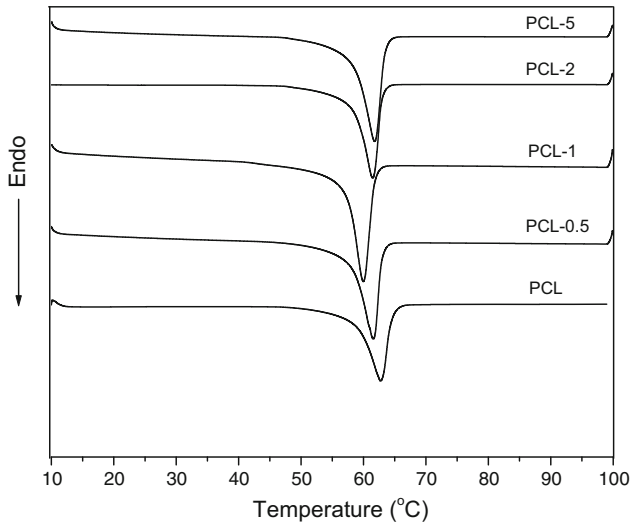

Figure 2 DSC melting endotherms of PCL and its composite scaffolds loaded with ZnO nanofiller.

Table 3 Thermal properties of the examined scaffolds determined by DSC

Sample	T_g (°C)[a]	T_m (°C)[a]	ΔH_m (J g^{-1})[a]	X_c of PCL (%)[a]
PCL	−61.5	62.7	89.1	63.8
PCL-0.5	−60.8	61.5	104.4	75.2
PCL-1	−61.1	59.9	102.4	74.1
PCL-2	−61.1	61.4	103.1	75.4
PCL-5	−60.9	61.7	107.4	81.0
	T_c (°C)	ΔH_c (J g^{-1})	X_c of PCL (%)	ΔT (°C)
PCL	30.8	53.6	38.4	26.8
PCL-0.5	31.7	61.2	44.1	24.7
PCL-1	33.1	62.3	45.1	23.4
PCl-2	32.3	61.7	45.1	24.7
PCL-5	35.2	62.8	47.4	20.9
		T_m (°C)[b]	ΔH_m (J g^{-1})[b]	X_c of PCL (%)[b]
PCL	–	57.6	51.3	36.7
PCL-0.5	–	56.5	60.3	43.4
PCL-1	–	56.6	63.9	46.2
PCL-2	–	56.5	62.6	45.7
PCL-5	–	56.7	63.6	47.9

[a] First melting runs

[b] Second melting runs

The DSC thermograms of the reheated samples show almost no changes in the melting temperatures ($T_m = 56$ °C), and significantly lower degrees of crystallinity for all investigated samples when compared to those, characteristic for the first heating runs (I). This could be an additional confirmation that the polymer's higher degrees of crystallinity (I runs) are exclusively due to the thermally induced phase-separation process and slow solvent extraction in frozen state, rather than nucleation effect of the nanofiller. The presented degrees of crystallinity in Table 3 (reheated samples) also showed good correlation with the data derived from the DSC crystallization runs.

FTIR characterization was performed to analyze the influence of nanoparticles on the crystalline sensitive bands of PCL. FTIR–ATR spectra of pure PCL and PCL/ZnO nanocomposite scaffolds are presented in Fig. 4. In the absorption spectrum of pure PCL scaffold, a characteristic band of C=O stretching is observed at 1721 cm^{-1}, and bands at 1471, 1396 and 1356 cm^{-1} arising from the CH_2 bending modes are identified [32, 33]. The bands corresponding to CH_2 asymmetric and symmetric stretching vibrations are positioned at 2945 and 2866 cm^{-1}, respectively. The stretching vibrations of C–O–C are found at 1045, 1107 and 1238 cm^{-1}, while the bands at 1166 and 1293 cm^{-1} are assigned due to C–O and C–C stretching vibrations in the amorphous and crystalline state, respectively [32, 33].

The addition of ZnO nanofiller does not have significant influence on the absorption spectra of composite scaffolds (band shifts) except certain changes in the characteristic peaks intensities are observed. In order to understand the influence of the nanofiller on PCL microstructure, crystallinity index (CI) was estimated as the ratio of peak intensities positioned at 1293 and 1166 cm^{-1} [34]. From the presented data (Table 4), it could be seen that with the increase in nanofiller content slightly increased crystallinity indices are identified. The last data are in close correlation with the data obtained from DSC measurements.

XRD patterns (Fig. 5) of the prepared scaffolds show two strong reflections at 2θ of about 21.3° and 23.5°, corresponding to the (110) and (200) planes of the orthorhombic PCL crystal structure, respectively [35]. The small reflection as a shoulder of the first peak (positioned at 2θ of 22°) corresponds to the (111) plane of the same crystal lattice. The composite scaffolds that exhibit additional reflections (designated with asterisk positioned at 2θ of 31.8°, 34.5°, 36.3°, 47.6° and 56°) are typical patterns of ZnO nanoparticles related to (100) (002), (101), (102) and

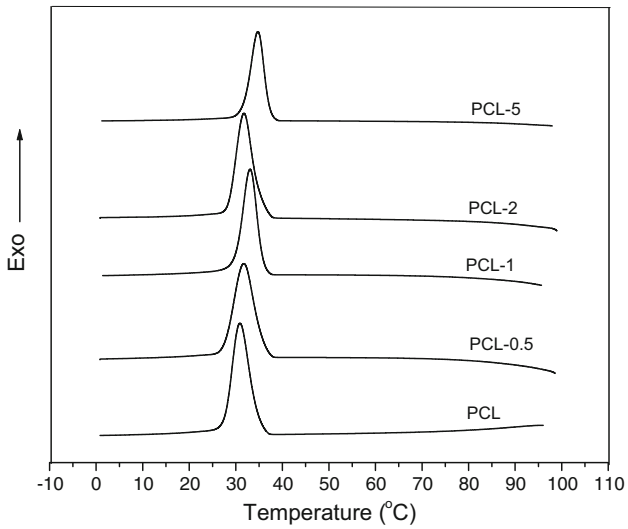

Figure 3 Crystallization exotherms for PCL/ZnO nanocomposite scaffolds.

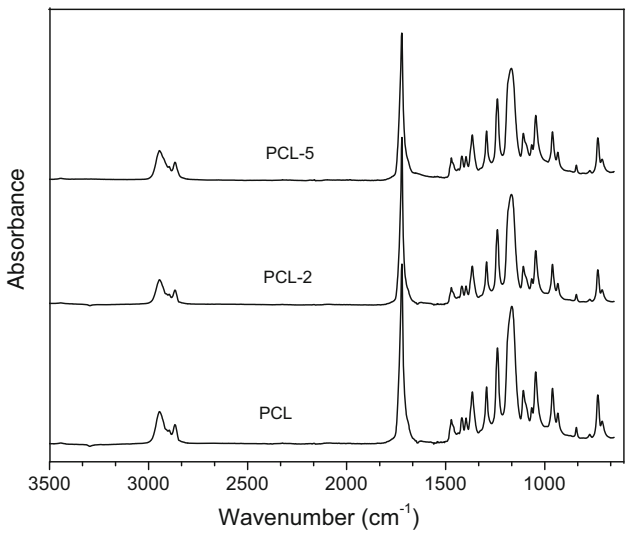

Figure 4 FTIR–ATR spectra of PCL and its composites loaded with ZnO nanofiller.

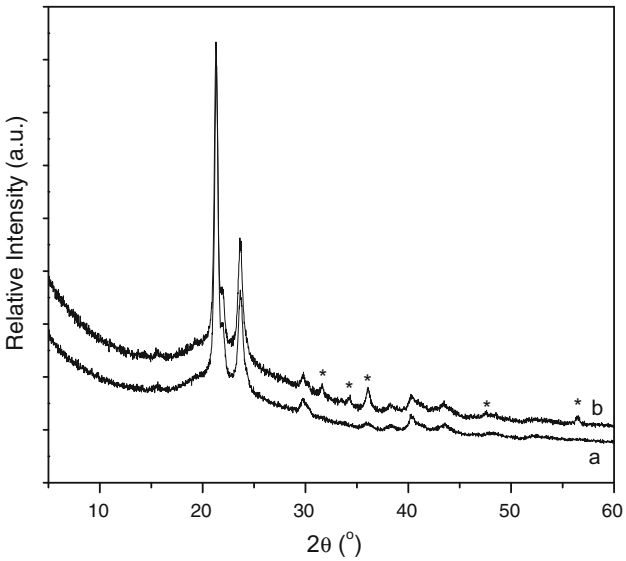

Figure 5 X-ray diffraction patterns of PCL (*a*) and PCL-0.5 (*b*) scaffolds. The *asterisks* highlight the characteristic reflections of ZnO nanofiller.

(110) planes correspondingly [36]. It could be noted that the main reflections of PCL matrix were not affected by the presence of nanofiller in different contents, thus suggesting that nanofiller does not change the polymer crystal organization.

Porosity and morphological characterization of the scaffolds

The porosity of the scaffolds produced by thermally induced phase-separation method is generally dependent of polymer concentration, the rate of cooling as well as freezing temperature [37, 38]. The higher polymer concentration in appropriate solvent as well as higher content of nanofiller generally leads

Table 4 Crystallinity and carbonyl indices of the PCL samples before and after incubation in simulated body fluid

Sample	CI (%)[a]	CI (%)[b]	CI (%)[c]	Carbonyl index (%)[b]	Carbonyl index (%)[c]
PCL	36	35	43	12.3	8.4
PCL-0.5	36	40	47	9.0	7.9
PCL-1	35	37	50	10.3	8.5
PCl-2	36	37	53	11.4	9.2
PCL-5	39	37	51	11.0	6.5

[a] CI for prepared polymer scaffolds

[b] Incubation time of 15 days in SBF

[c] Incubation time of 30 days in SBF

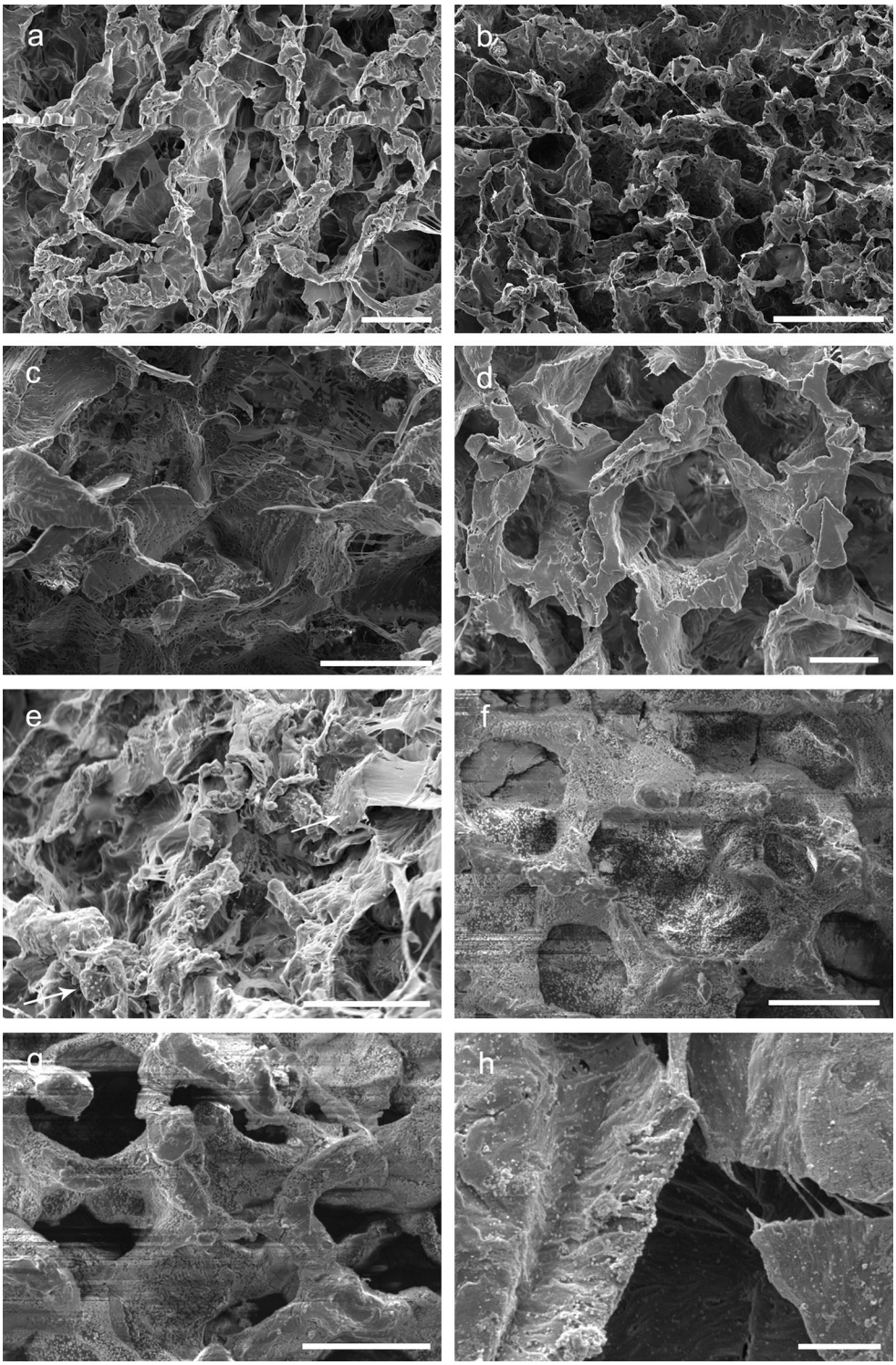

Figure 6 SEM images of the morphology of the PCL (**a**), PCL-0.5 (**b**), PCL-1 (**c**) and PCL-5 (**d**) scaffolds and SEM images after their incubation in SBF for 30 days; PCL (**e**) PCL-0.5 (**f**), PCL-1 (**g**) and PCL-5 (**h**) at different magnifications. *Scale bars* **b**, **c** = 50 μm; **a**, **d**, **e**–**g** = 20 μm; **h** = 10 μm.

to lower porosity of the produced scaffolds. The measured porosities in all investigated PCL scaffolds were in the range between 90 and 92%, with insignificant influence of the nanofiller on the measured values. The relatively low ZnO contents between 0.5 and 5 wt% related to PCL were not

expected to change the total porosity of the scaffolds. Similar porosities were obtained for PLA scaffolds produced by TIPS fabrication procedure at similar polymer concentrations in dioxane [39].

SEM microscopy was used to analyze the morphology of the prepared scaffolds. SEM images of PCL nanocomposite scaffolds are shown in Fig. 6a–d. A highly porous, anisotropic architecture could be seen in all investigated composite scaffolds with characteristic interconnected and elongated pores with lengths in the range between 40 and 90 μm and variable walls thickness depending on the ZnO content. As the content of nanofiller increased, thicker walls up to 6 μm were observed, for example in PCL-5 composite scaffold. Nanofiller content of 0.5–5 wt% seems to have no significant influence on the pore architecture, as it was also confirmed by the porosity measurements. The nanoparticles are visible as white dots within the polymer matrix only for their higher content of 5 wt% (PCL-5). Namely, the TIPS fabrication method leads to production of polymer scaffolds with well-dispersed nanofiller as it was reported in a previous research [40]. Such a behavior, i.e., very well distribution of the nanofiller within the polymer matrix, could be ascribed to the fact that the freezing process (during the scaffolds preparation) does not allow the formation of larger agglomerates in the viscous PCL dioxane solutions.

Bioactivity evaluation and degradation of PCL/ZnO scaffolds in SBF

The in vitro bioactivity of the certain scaffolds is usually assessed by the induced hydroxyapatite (HAp) formation, when treating the samples in simulated body fluid (SBF). Usually different solutions have been used for testing the scaffolds bioactivity, such as standard SBF solutions [25] or super saturated Ca/P solutions for fast bioactivity testing [41]. In this paper, standard SBF was used in order to evaluate the bioactivity of PCL/ZnO nanocomposite scaffolds and at the same time to follow their degradation behavior, as an important issue when using these materials for tissue engineering applications.

There was no evidence of induced hydroxyapatite, examined with SEM, in all tested scaffolds, after incubation period of 15 days. SEM micrographs of the SBF treated scaffolds for 30 days are presented in Fig. 6e–h. It is obvious that the appearance of apatite dots is rarer in pure PCL scaffold (denoted with arrows) when compared with the SEM micrographs of the PCL/ZnO nanocomposite samples. The SEM images of PCL-0.5 and PCL-1 scaffolds show the mineralization at the surface and the inner parts of the scaffold body. Less pronounced apatite particles were identified in PCL-5 nanocomposite scaffold, suggesting that the increased ZnO content promotes lower level of mineralization. Further evidence of

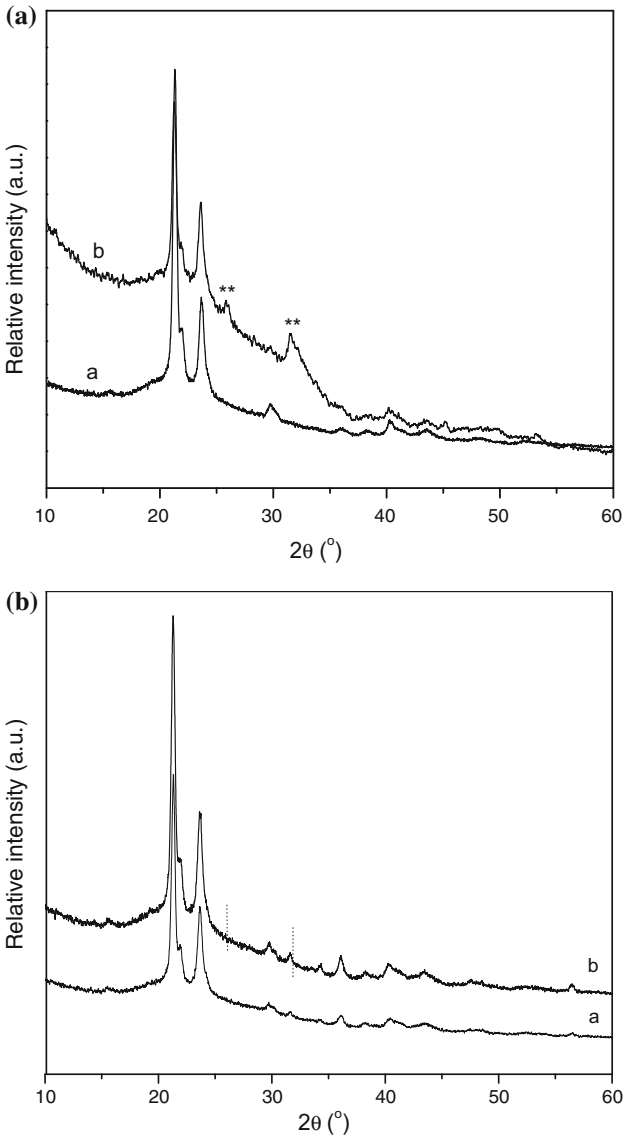

Figure 7 **a** XRD patterns of PCL before (*a*) and after incubation in SBF for 30 days, (*b*) *double asterisk* highlights the two main reflections $2\theta = 26°$ and 32°, characteristic for hydroxyapatite. **b** XRD patterns of PCL-0.5 scaffolds before (*a*) and after incubation in SBF for 30 days (*b*). *The dashed bars* indicate the position of hydroxyapatite reflections superimposed with the characteristic peaks of ZnO.

hydroxyapatite formation was given by XRD measurements. XRD diffractograms of the pure PCL and PCL-0.5 scaffolds treated for 30 days in SBF are shown in Fig. 7a, b. New reflections positioned at 2θ of 26° and 32° characteristic for HAp [42] could be identified only in PCL treated scaffolds, while for the other nanofilled composites the apatite reflections are superimposed with the reflections corresponding to the ZnO nanoparticles. From this point of view, it was difficult to distinguish the additional reflexes

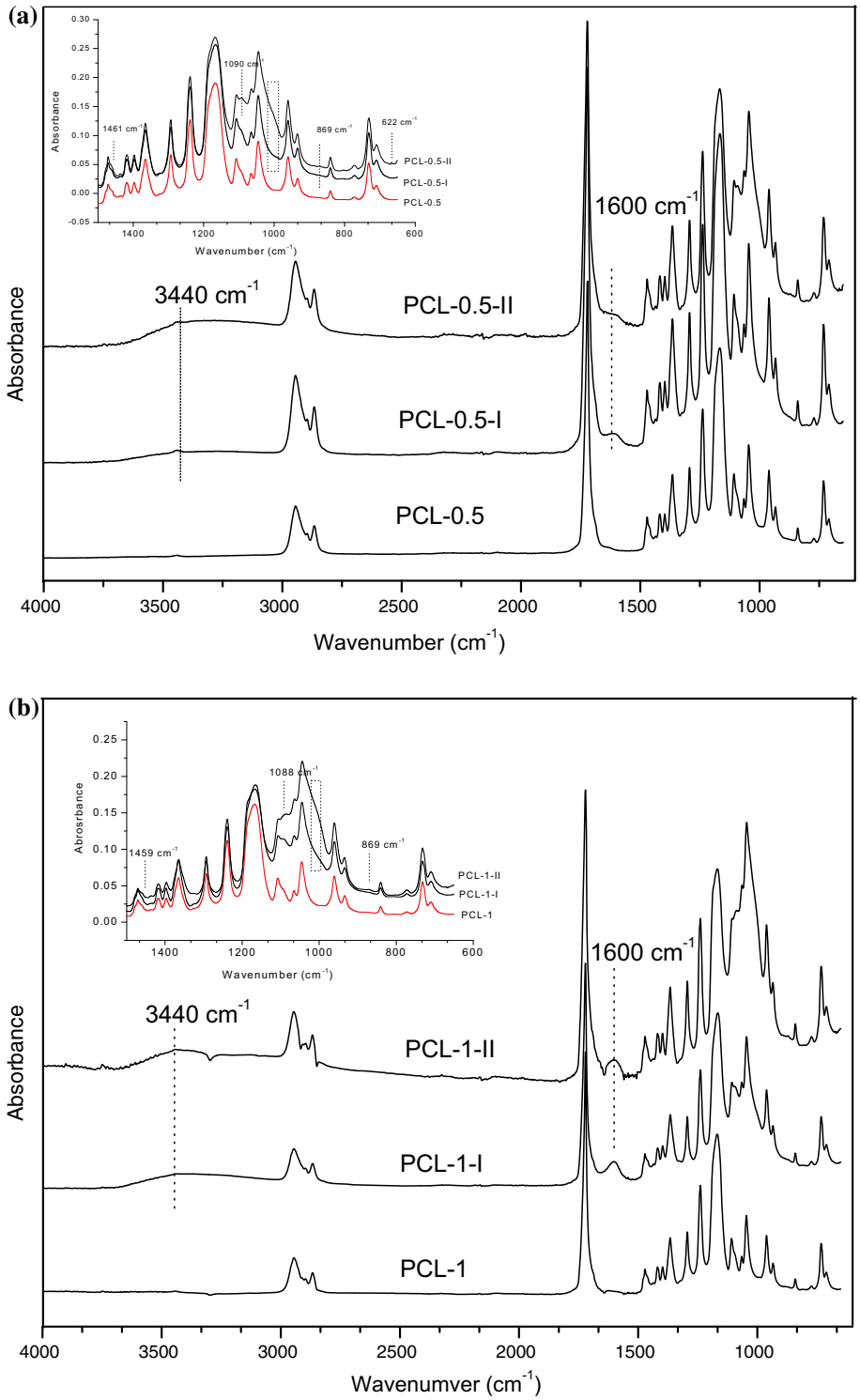

Figure 8 **a** FTIR spectra of PCL-0.5, PCL-0.5-I (incubated in SBF for 15 days) and PCL-0.5-II (incubated in SBF for 30 days) scaffolds. **b** FTIR spectra of PCL-1, PCL-1-I (incubated in SBF for 15 days) and PCL-1-II (incubated in SBF for 30 days) scaffolds.

related to crystalline hydroxyapatite in ZnO-filled scaffolds by XRD.

The FTIR spectra of PCL/ZnO nanocomposites after immersion in SBF for 15 and 30 days are illustrated in Fig. 8a, b. It could be seen that new bands positioned at 3440, 1461, 1600, 1090 and band around 1033, 869 and 622 cm^{-1} are identified. The appearance of the absorption band at 3440 cm^{-1} is connected to the stretching mode of OH groups in HAp, while the bands at 1090 and around 1033 cm^{-1} arise from PO_4^{3-} vibrations [43]. The presence of band located at around 1600 cm^{-1} could suggest the formation of carbonated apatite on the surface of polymer scaffolds. The evidence of carbonated apatite is also proved by the appearance of the band located at 1460 cm^{-1}, which is actually due to the asymmetric stretching of CO_3^{2-}. It should be underlined that the main vibration bands (v_3) of PO_4^{3-} ions, located at around 1033 cm^{-1}, are usually overlapped with the PCL characteristic bands. It is interesting to point out that these characteristic bands are more pronounced (in intensity) in PCL-0.5, PCL-1 and PCL-2 scaffolds treated for 30 days in SBF. For PCL-5 samples, less intensive characteristic bands were identified, suggesting restricted mineralization process.

The mineralization process of all investigated scaffolds was quantified by TGA measurements. The results obtained from TGA analysis of all treated scaffolds in SBF (for 30 days) are presented in Table 2. It could be observed that the quantity of HA determined as weight residue (the total weight residue was reduced for the relevant nominal values of loaded ZnO) at 600 °C ranged between 1.9 and 1.1 wt%, depending on the nanofiller content. The highest weight residue of 1.9% was determined for PCL-0.5 scaffold, while by increasing the content of ZnO (for example PCL-5-II), the weight residue percent decreased, confirming the reduced mineralization process. Even a small quantity of the nanofiller (0.5 wt%) generally accelerates HAp formation probably to its best distribution within the polymer matrix. PCL degradation process in SBF fluid was followed by the changes in CI as well as the carbonyl index defined as the ratio of the peak intensities corresponding to carbonyl stretching at 1722 cm^{-1} and CH_2 bending at 1420 cm^{-1} [34]. All relevant data of the determined crystalline and carbonyl indices for the treated scaffolds in SBF (15 and 30 days) are shown in Table 4. Sample scaffolds treated for 15 and 30 days showed increased crystallinity indices with the increase in the time of immersion in SBF and nanofiller content. This could be another confirmation that degradation occurred during the SBF treatment. Actually the degradation primarily occurs in amorphous regions of the polymer matrix, thus increasing the total crystallinity of the system [44]. As it could be seen, the estimated carbonyl indices, showed decreasing tendency with the prolonged time of scaffolds immersion in SBF (pH 7.25), giving an additional confirmation that the degradation process of PCL matrix proceeds through the hydrolysis of carbonyl bonds. The process of hydrolysis of ester bonds is usually connected with the formation of OH and COOH groups [45]. After being hydrolyzed by water molecules in SBF, the COOH groups in PCL dissociate into carboxylate anions which can be combined with the calcium and phosphates ions, thus forming the hydroxyapatite phase.

The creation of functional groups as a result of hydrolysis process could explain the formation of HAp even in unloaded PCL scaffold. Their presence in PCL/ZnO composites (besides the existence of OH surface groups of ZnO nanofiller) could additionally support the mineralization process (higher-weight residues were determined by TGA). Anyway these small differences in the weight residues could be due to the fact that by treating the polymer scaffolds in SBF, hydrolysis is observed in all samples, creating functional groups essential for HP formation.

Conclusions

PCL/ZnO nanocomposite scaffolds with different contents of nanofiller (between 0.5 and 5 wt%) were prepared by thermally induced phase-separation method using freeze solvent extraction with ethanol.

SEM micrographs of all produced scaffolds showed anisotropic morphology with elongated pores and dimensions between 40 and 90 μm, characteristics which are relevant for tissue engineering applications. High porosity of around 92% was determined in all fabricated scaffolds independently of the nanofiller content.

The investigated scaffolds showed decreased thermal stability with the increase in ZnO content due to its negative catalytic effect. The thermally induced phase-separation method was proved as a procedure that leads to significantly high degree of crystallinity (X_c between 63 and 81%, depending on

the nanofiller content) besides the slight nucleation capacity of the ZnO nanofiller. FTIR spectroscopy and XRD measurements of the prepared scaffolds confirmed that the nanofiller did not alter the structure of the polymer matrix.

By immersing the PCL/ZnO scaffolds in SBF for 30 days, bioactivity was confirmed in all systems. The weight residues (determined at 600 °C by TGA analysis) indicated highest level of mineralization in scaffolds with lower content of ZnO (between 0.5 and 1 wt%).

Acknowledgements

The author of the paper would like to acknowledge Dr. Zarah Walsh-Korb (University of Strasbourg) for her assistance in performing the SEM observations.

Electronic supplementary material: The online version of this article (doi:10.1007/s10853-017-1342-9) contains supplementary material, which is available to authorized users.

References

[1] Armentano I, Dottori M, Fortunati E, Mattioli S, Kenny JM (2010) Biodegradable polymer matrix nanocomposite for tissue engineering: a review. Polym Degrad Stab 95:2126–2146

[2] Armentano I, Bitinis N, Fortunati E, Mattioli S, Rescignano N, Verdejo R, Lopez-Mmanchado MA, Kenny JM (2013) Multifunctional nanostructured PLA materials for packaging and tissue engineering. Prog Polym Sci 38:1720–1747

[3] Ruiz-Hitzky E, Fernandes FM (2013) Progress in bio-nanocomposites: from green plastics to biomedical applications. Prog Polym Sci 38:1389–1772

[4] Ali SAM, Zhong SP, Doherty PJ, Williams DF (1993) Mechanisms of polymer degradation in implantable devices. I. Poly(caprolactone). Biomaterials 14:648–656

[5] Diba M, Kharaziha M, Fathi MH, Gholipourmlekabadi M, Samadikuchaksaraei A (2012) Preparation and characterization of polycaprolactone/forsterite nanocomposite porous scaffolds designed for bone tissue engineering. Compos Sci Technol 72:716–723

[6] Li WJ, Tuli R, Okafor C, Derfoul A, Danielson KG, Hall DJ, Tuan RS (2005) A three-dimensional nanofibrous scaffold for cartilage tissue engineering using human mesenchymal stem cells. Biomaterials 26:599–609

[7] Ulery BD, Nair LS, Laurencin CT (2011) Biomedical application of biodegradable polymers. J Polym Sci B Polym Phys 49:832–864

[8] Seretouidi G, Bikiaris D, Panayiotou C (2002) Synthesis, characterization and biodegradability of poly(ethylene succinate)/poly(ε-caprolactone) block copolymers. Polymer 43:5405–5415

[9] Ródenas-Rochina J, Ribelles JL, Lebourg M (2013) Comparative study of PCL-HAp and PCL-bioglass composite scaffolds for bone tissue engineering. J Mater Sci Med 24:1293–1308

[10] Cannillo V, Chiellini F, Fabbri P (2010) Production of Bioglass® 45S5—polycaprolactone composite scaffolds via salt-leaching. Compos Struct 92:1823–1832

[11] Chuenjitkuntaworn B, Inrung W, Damrongsri D, Mekaapiruk K, Supaphol P, Pavasant P (2010) Polycaprolactone/hydroxyapatite composite scaffolds: production, characterization, and in vitro and in vivo biological responses of human primary cells. J Biomed Mater Res A 94:241–251

[12] Msdhsvan RV, Rosemary MJ, Nadkumar MA, Krishnan KV, Krishnan LK (2011) Silver nanoparticle impregnated poly(ε-caprolactone) scaffolds: optimization of antimicrobial and noncytotoxic concentrations. Tissue Eng Part B 17:439–449

[13] Crowder SW, Liang Y, Rath R, Park AM, Maltais S, Pintauro PN, Hofmeister W, Lim CC, Wang X, Sung HJ (2013) Poly(ε-caprolactone)-carbon nanotube composite scaffolds for enhanced cardiac differentiation of human mesenchymal stem cells. Nanomedicine 8:1763–1776

[14] Goreham RV, Mierczynska A, Smith LE, Sedev R, Vasilev K (2013) Small surface nanotopography encourages fibroblast and osteoblast cell adhesion. RSC Adv 3:10309–10317

[15] Zhang Y, Nayak TR, Hong H, Cai W (2013) Biomedical applications of zinc oxide nanomaterials. Curr Mol Med 13:1633–1645

[16] Treccani L, Klein TY, Meder F, Pardun K, Rezwan K (2013) Functionalized ceramics for biomedical and environmental applications. Acta Biomater 9:7115–7150

[17] Augustine R, Malik HN, Singhal DK, Mukherjee A, Malakar D, Kalarikkal N, Thomas S (2014) Electrosun polycaprolactone/ZnO nanocomposite membranes as biomaterial with antibacterial and cell adhesion properties. J Polym Res 21:347–364

[18] Augustine R, Dominic EA, Reju I, Kaimal B, Kalarikkal N, Thomas S (2014) Investigation of angiogenesis and its mechanism using zinc oxide nanoparticle-loaded electrospun tissue engineering scaffolds. RSC Adv 4:51528–51536

[19] Münchow EA, Albuquerque MTP, Zero B, Kamocki K, Piva E, Gregory RL, Bottino MC (2015) Development and characterization of novel ZnO-loaded electrospun membranes for periodontal regeneration. Dent Mater 31:1038–1051

[20] Kim J, Mousa HM, Park CH, Kim CS (2017) Enhanced corrosion resistance and biocompatibility of AZ31 Mg alloy using PCL/ZnO NPs via electospinning. Appl Surf Sci 396:249–258

[21] Abedalwafa M, Wang F, Wang L, Li C (2013) Biodegradable poly-epsilon-caprolactone (PCL) for tissue engineering applications: a review. Rev Adv Mater Sci 34:123–140

[22] Ge Z, Jin Z, Cao T (2008) Manufacture of degradable polymeric scaffolds for bone regeneration. Biomed Mater 3:022001. doi:10.1088/1748-6041/3/2/022001

[23] Gualandi C, Govoni M, Foroni L, Valente S, Bianchi M, Giordano E, Pasquinelli G, Biscarini F, Focarete ML (2012) Ethanol disinfection affects physical properties and cell response of electrospun poly(L-lactic acid) scaffolds. Eur Polym J 48:2008–2018

[24] Ho MH, Kuo PY, Hsieh HJ, Hsien TY, Hou LT, Lai JY, Wang DM (2004) Preparation of porous scaffolds by using freeze-extraction and freeze-gelation methods. Biomaterials 25:129–138

[25] Kokubo T, Kushitani H, Sakka S, Kitsugi T, Yamamuro T (1990) Solutions able to reproduce in vivo surface-structure changes in bioactive glass–ceramic A–W. J Biomed Mater Res A 24:721–734

[26] Kothapalli CR, Shaw MT, Wei M (2005) Biodegradable HA-PLA 3D porous scaffolds: effect of nano-sized filler content on scaffolds properties. Acta Biomater 1:653–662

[27] Crescenzi V, Mancini G, Calzolari G, Borri C (1972) Thermodynamics of fusion of poly-β-propiolactone and poly-ε-caprolactone. Comparative analysis of the melting of aliphatic polylactone and polyester chains. Eur Polym J 8:449–463

[28] Peng H, Han Y, Liu T, Tjiu WC, He C (2010) Morphology and thermal degradation behaviour of highly exfoliated CoAl-layered double hydroxide/polycaprolactone nanocomposites prepared by simple solution intercalation. Thermochim Acta 502:1–7

[29] Liu JY, Reni L, Wei Q, Wu JL, Liu S, Wang YJ, Li GY (2011) Fabrication and characterization of caprolactone/calcium sulfate whisker composites. Express Polym Lett 5:742–752

[30] Augustine R, Nandakumar K, Thomas S (2016) Effect of zinc oxide nanoparticles on the in vitro degradation of electrospun polycaprolactone membranes in simulated body fluid. Int J Polym Mater 65:28–37

[31] Mandelkern L (2004) Crystallization of polymers: kinetics and mechanisms, vol 2, 2nd edn. Cambridge University Press, Cambridge

[32] Coleman MM, Zarian J (1979) Fourier-transform infrared studies of polymer blends. II. Poly(a-caprolactone)-poly(vinylchloride) system. Polym Sci Polym Phys Ed 17:837–850

[33] Elzein T, Nasser-Eddine M, Delaite C, Bistac S, Dumas P (2004) FTIR study of polycaprolactone chain organization at interfaces. J Colloid Interface Sci 273:381–387

[34] He Y, Inoue Y (2000) Novel FTIR method for determining the crystallinity of poly(ε-caprolactone). Polym Int 49:623–626

[35] Chen EC, Wu TM (2007) Isothermal crystallization kinetics and thermal behavior of poly(-caprolactone)/multi-walled carbon nanotube composites. Polym Degrad Stab 92:1009–1015

[36] Chen C, Yu B, Liu P, Liu JF, Wang L (2011) Investigation of nano-sized ZnO particles fabricated by various synthesis routes. J Ceram Process Res 12:420–425

[37] Hu X, Shen H, Yang F, Bei J, Wang S (2008) Preparation and cell affinity of microtubular oriented-structured PLGA(70/30) blood vessel scaffold. Biomaterials 29:3128–3136

[38] Yang F, Qu X, Cui W, Bei J, YuF LuS, Wang S (2006) Manufacturing and morphology structure of polylactide-type microtubules orientation-structured scaffolds. Biomaterials 27:4923–4933

[39] Ma PX, Zhang R (2001) Microtubular architecture of biodegradable polymer scaffolds. J Biomed Mater Res 56:469–477

[40] Buzarovska A, Gualandi C, Parrilli A, Scandola M (2015) Effect of TiO_2 nanoparticle loading on Poly(L-lactic acid) porous scaffolds fabricated by TIPS. Compos Part B 81:189–195

[41] Bracci B, Panzavolta S, Bigi A (2013) A new simplified calcifying solutions to synthesize calcium phosphate coatings. Surf Coat Technol 232:13–21

[42] Powder Diffraction File n. 9-432, International Center for Diffraction Data (ICDD), Newtown Square, PA USA

[43] Berzina-Cimdina L, Borodajenko N (2012) Research of calcium phosphates using Fourier infrared spectroscopy. In: Theophanidis T (ed) Infrared spectroscopy—materials science, engineering and technology. InTech, pp 123–148

[44] Chang HM, Prasannan A, Tsai HC, Jhu JJ (2014) Ex vivo evaluation of biodegradable poly(e-caprolactone) films in digestive fluids. Appl Surf Sci 313:828–833

[45] Wei J, Chen QZ, Stevens MM, Roether JA, Boccaccini AR (2008) Biocompatibility and bioactivity of PDLLA/TiO_2 and PDLLA/TiO_2/Bioglass nanocomposites. Mater Sci Eng 28:1–10